Interaction between Tetramethylcucurbit[6]uril and Some Pyridine Derivates

Hang Cong,[†,‡] Long-Ling Tao,[§] Yi-Hua Yu,[§] Zhu Tao,*[,†] Fan Yang,*[,‡] Yun-Jie Zhao,[†] Sai-Feng Xue,[†] Geoffrey A. Lawrance,*[,||] and Gang Wei*[,⊥]

Institute of Applied Chemistry, Guizhou University, Guiyang, Guizhou 550025, P. R. China, Department of Chemistry, East China Normal University, Shanghai 200062, P. R. China, Key Laboratory of Optical and Magnetic Resonance Spectroscopy of Ministry of Education, East China Normal University, Shanghai 200062, P. R. China, Discipline of Chemistry, School of Environment and Life Science, the University of Newcastle, Callaghan, NSW 2308, Australia, and CSIRO Industrial Physics, P.O. Box 218, Lindfield NSW 2070, Australia

Received: September 15, 2006; In Final Form: January 24, 2007

Interaction between tetramethylcucurbit[6]uril (TMeQ[6], host) with hydrochloride salts of 2-phenylpridine (**G1**), 2-benzylpyridine (**G2**), and 4-benzylpyridine (**G3**) (guests) have been investigated by using ^{1}H NMR spectroscopy and electronic absorption spectroscopy and theoretical calculations. The ^{1}H NMR spectra analysis established an interaction model in which the host selectively included the phenyl moiety of the HCl salt of the above three guests, and formed inclusion complexes with a host−guest ratio of 1:1. Absorption spectrophotometric analysis allowed quantitative measurement of the stability of these host−guest inclusion complexes. Particularly, we have established a competitive interaction in which one host−guest inclusion complex pair is much more stable than another host−guest inclusion complex pair. The stability constants for the three host−guest inclusion complexes of TMeQ[6]-**G1**, TMeQ[6]-**G2**, and TMeQ[6]-**G3** are $\sim 2 \times 10^6$, 60.7, and 19.9 mol^{-1}·L, respectively. To understand how subtle differences in the structure of the title guests lead to a significant difference in the stability of the corresponding host−guest inclusion complexes with the TMeQ[6], ab initio theoretical calculations have been performed, not only for the gas phase but also the solution phase (water as solvent) in all cases. The calculation results revealed that when the phenyl moiety of the three pyridine derivate guests was included, the host−guest complexation reached the minimum, and the corresponding energy differences for the formation of the title host−guest inclusion complexes are qualitatively consistent with the experimental results.

Introduction

Cucurbit[*n*]urils are relatively new members in the macrocyclic compound family; they are made of glycoluril units interconnected with methylene bridges and have a macrocyclic cage rimmed by a number of carbonyl oxygens. The novel structure and a capability for forming complexes with molecules and ions make the cucurbit[*n*]uril family attractive, not only as a synthetic receptor but also as a building block for supramolecular assemblies such as rotaxanes, catenanes, and molecular machines.[1−7] To date, the normal cucurbit[*n*]uril family has 5 homologues abbreviated as Q[5], Q[6], Q[7], Q[8], and Q[10] (Qs) according to the cyclization monomer numbers.[8−11] In recent years, a series of cucurbit[*n*]uril derivatives have been synthesized by introducing alkyl groups at the equator of the Qs to improve their solubility in water and common organic solvents; examples are the fully substituted cyclohexanocucurbit[*n*]urils ($n = 5, 6$) with an improved solubility in water and some organic solvents[12] and some partially substituted cucurbit[*n*]urils with not only a good solubility but also preparable in good yields.[13−18] Some reactive functional groups have been introduced directly on the surface of the Qs and their analogues for improving the solubility as well as for further modification such as the perhydroxycucurbit[5]uril, perhydroxycucurbit[6]uril,[20] and some cucurbit[*n*]uril analogues substituted by CO_2Et, CO_2H, and $CO_2(CH_2)_9CH_3$ groups.[21−23] More recently, the disclosure of some inverted cucurbit[*n*]urils and hemicucurbit[*n*]urils had further increased the members in the Q[*n*]s family.[24,25]

The members in the Q[*n*]s family have common characteristic features, i.e., a hydrophobic cavity and two opening hydrophilic portals. In addition, the varying cavity and portal sizes lead to the ability of the Q[*n*]s to form inclusion or exclusion complexes with different organic or inorganic species through a combination of dipole−ion, hydrogen bonding, and hydrophobic interactions, and these achievements have been summarized in different reviews in different periods of development of Q[*n*]s chemistry.[1−7] Among them, the interaction of host−guest complexes of different Q[*n*]s with a number of positively charged organic guests, particularly the protonated alkyl or aromatic amines, pyridine and its derivatives, phenanthroline and its derivatives, and so on, have been extensively investigated and the combined dipole−ion, hydrogen bonding, and hydrophobic interactions have been studied in detail.[26−37]

In this work, HCl salts of 2-phenylpridine (**G1**), 2-benzylpridine (**G2**), and 4-benzylpridine (**G3**) have been chosen for investigating the interaction behavior with a water-soluble partially substituted cucurbit[6]uril, tetramethylcucurbit[6]uril (TMeQ[6]).[16] The three guests containing two moieties, phenyl and pyridyl, exhibit a similar structure (Figure 1); there is a

* To whom correspondence should be addressed. E-mail: ecnuc@163.com (Z.T.); fyang1@chem.ecnu.edu.cn (F.Y.); Geoffrey.Lawrance@newcastle.edu.au (G.A.L.); gang.wei@csiro.au (G.W.). Telephone: +86 851 3623 903 (Z.T.).

† Guizhou University.

‡ East China Normal University.

§ Key Laboratory of Optical and Magnetic Resonance Spectroscopy.

|| The University of Newcastle.

⊥ CSIRO, Industrial Physics.

10.1021/jp066031j CCC: $37.00 © 2007 American Chemical Society
Published on Web 03/22/2007

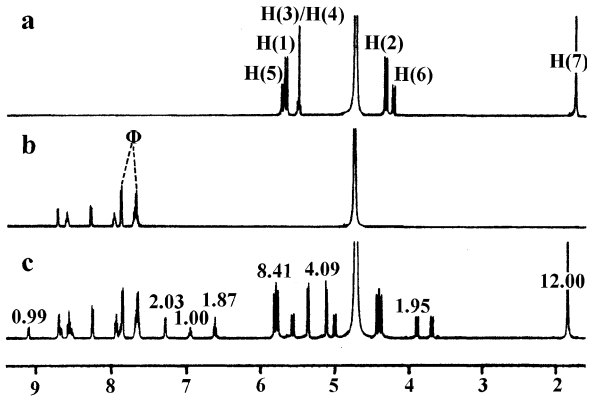

Figure 1. ^{1}H NMR spectra of (a) TMeQ[6], (b) guest **G1**, and (c) TMeQ[6]-**G1** ($C_{TMeQ[6]}/C_{G1}$ = 1:2.5). *x* axis: chemical shift (ppm). *y* axis: intensity of resonance. Φ: resonances of phenyl protons of the guest. In (c) the intensities of the corresponding protons are given.

bridged methylene between phenyl and pyridyl in guests **G2** or **G3**, and the position of the pyridyl nitrogen in **G2** or **G3** is different. In previous work, we found that both phenyl and pyridyl could be readily included in cavity of Q[6] and its derivatives.[36,37] ^{1}H NMR spectroscopy reveals that the host TMeQ[6] selectively included the phenyl moiety when the phenyl and pyridyl moieties are in the same guest and formed an inclusion complex with a host−guest ratio of 1:1. ^{1}H NMR spectroscopy and electronic absorption spectroscopy analysis indicated that the host−guest inclusion complex of TMeQ[6]-**G1** was the most stable one. The theoretical calculation using HF (Hatree−Fock)/3-21G* standard basis sets further confirmed the experimental results and gives a quantitatively determined order of stability of the three host−guest inclusion complexes of TMeQ[6]-**G1** > TMeQ[6]-**G2** > TMeQ[6]-**G3**.

Experimentation and Computational Methods

TMeQ[6], which can formed the stable inclusion complexes with 2,2'-bipyridine or 2-(aminomethyl)pyrine,[17,19] was prepared and purified according to the methods developed in our laboratory.[17] All guests were purchased from Aldrich and used without further purification. The corresponding HCl salts of the guests **1**, **2**, and **3** (hereafter **G1, G2**, and **G3)** were prepared by dissolving the pyridines in 10 M HCl, followed by crystallization with ethanol or acetone addition, collecting them by filtration and drying.

For the study of host−guest complexation of TMeQ[6] and the title guests, 2.0−2.5 × 10^{-3} mmol samples of TMeQ[6] in 0.5−0.7 g D_2O with [guest]/[TMeQ[6]] ranging between 1 and 100 were prepared. The ^{1}H NMR spectra were recorded at 300 K on a Bruker 500 MHz spectromete.

Absorption spectra of the host−guest complexes were recorded on a Unico UV-2102 instrument at 25 °C. For the TMeQ[6]-G1 system, aqueous solutions of **G1** and TMeQ[6] were prepared with a concentration of 1.00 × 10^{-4} mol·L^{-1} and 2.50 × 10^{-5} mol·L^{-1}, respectively, and samples of these solutions were combined to give solutions with a guest/TMeQ[6] ratio of 0, 8:1, 4:1, 2:1, 1:1, and 1:2 and so on. The spectrophotometric titrations were carried out at λ_{max} = 292 nm (ϵ = 1.20 × 10^4 L·mol^{-1}·cm^{-1}). For the TMeQ[6]-**G2** and TMeQ[6]-**G3** systems, the aqueous solutions of **G2**, **G3**, and TMeQ[6] were all prepared with a concentration of 2.00 × 10^{-4} mol·L^{-1}. Kinetic data for competitive interaction between the free guest **G1** with a combined host−guest of TMeQ/[6]**G2** or TMeQ[6]**G3** in a ratio of 1:1 was recorded at λ_{max} = 288 nm for 24 h.

All computational studies were performed using Hyperchem release 7.52[39] and Guassian 03W (revision C.02) software packages.[40] The initial structural detail for the TMeQ[6] and the free guests were built up using INDO/1 in the Hyperchem program. On the basis of these pre-optimization results, the basis set HF/3-21G* have been used for higher-level calculations. The pregeometry optimization of the host−guest inclusion complexes was established using an anneal method of molecular dynamics within the MM+ force field in the Hyperchem program, and the basis set HF/3-21G* has been used for higher-level calculations. The Onsager model was used to calculate the solvent effect as part of this computing package.

Results and Discussion

A. ^{1}H NMR Studies of the Interaction between TMeQ[6] and Guest Hydrochloride Salts. The examination of D_2O solutions of the host TMeQ[6], the guest **G1**, and the host−guest inclusion complex TMeQ[6]-**G1** by ^{1}H NMR spectroscopy showed that an inclusion complex was formed with slow exchange (Figure 1a−c). TMeQ[6] has D_{2h} symmetry, which results in a relatively simple ^{1}H NMR spectrum (Figure 1a). Referring to the labeled structure in Scheme 1, the protons H(2) and H(6) at 4.20 and 4.10 ppm, respectively, are doublets in a ratio of 2:1, consistent with the symmetrical TMeQ[6] structure. The inner ring H(2) protons of the methylene bridges adjacent to the dimethylglycoluril moiety are chemically equivalent and constitute eight of the total of 12 inner protons. The remaining four protons are attributed to H(6). The corresponding set of outer ring methylene proton resonances for H(1) and H(5) appear

SCHEME 1: Structures of TMeQ[6] Host and Guests

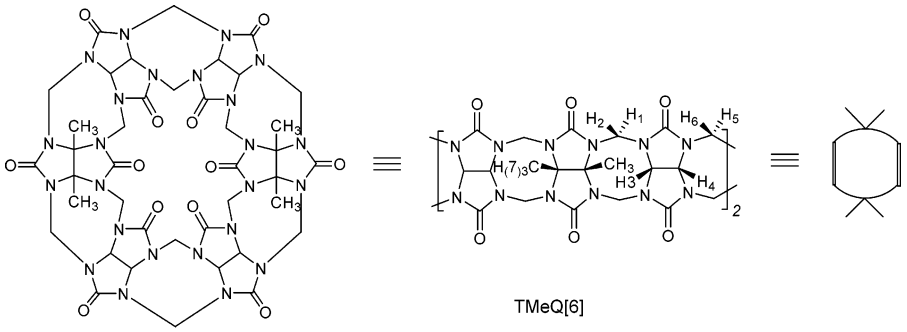

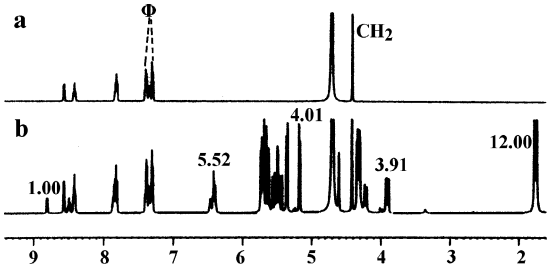

Figure 2. ^{1}H NMR spectra of (a) guest **G2** and (b) TMeQ[6]-**G2** ($C_{TMeQ[6]}/C_{G2}$ = 1:2.5). *x* axis: chemical shift (ppm). *y* axis: intensity of resonance. Φ: resonances of phenyl protons of the guest. In (b) the intensities of the corresponding protons are given.

as two overlapping doublets centered at 5.56 ppm. The methine protons H(3) and H(4) resonate at 5.38 ppm as an unusual triplet integrating for eight protons. The methyl protons H(7) are all equivalent and give a singlet at 1.64 ppm, integrating for 12 protons. The two ^{1}H NMR spectra (Figure 1b,c) of the free **G1** guest and TMeQ[6] with guest **G1** show the difference of bound and unbound guest as the ratio of the guest is increased to ~1:2.5. It is clearly evident in Figure 1c that the two aromatic rings of **G1** lie in different magnetic environments. The phenyl ring set of proton resonances at 6.61 (triplet), 6.93 (triplet), and 7.29 (doublet) ppm move upfield of the phenyl ring of the unbound **G1** proton resonances at 7.61 (two overlapped triplets) and 7.78 (doublet) ppm, while the pyridyl ring set of proton resonances at 9.11 (doublet), 8.69 (doublet) ppm move downfield of the pyridyl ring of the unbound **G1** proton resonances at 8.74 (doublet) and 8.24 (doublet) ppm; there is no obvious change for the two triplet proton resonances on the pyridyl. These obervations indicate that the phenyl ring of **G1** is contained within the cavity, whereas the pyridyl ring is left outside the cavity near the portal (upfield and downfield, respectively). The integral of bound **G1** relative to TMeQ[6] shows that an inclusion complex was formed with a TMeQ[6] to **G1** in a ratio of 1:1.

The ^{1}H NMR spectra of **G2** (Figure 2a) and TMeQ[6]-**G2** (Figure 2b) ($C_{TMeQ[6]}/C_{G2} \cong$ 1:2.5) show a similar inclusion model as that of TMeQ[6] with **G1**. The proton resonances of the phenyl of the bound **G2** move upfield by ~1.0 ppm from ~7.4 to ~6.4 ppm, and two proton resonances of the pyridyl of the bound **G2** move downfield by ~0.08 and 0.25 ppm, respectively. The methylene proton resonance of the **G2**, affected by deshielding of the portal of TMeQ[6], moves downfield from 4.51 to 4.73 ppm. This indicates that only the phenyl ring of the benzyl of the **G2** certainly enter the cavity of TMeQ[6]. Unlike the bound **G1**, the proton resonances of the included phenyl ring of **G2** appear at almost the same position, which suggests that the phenyl ring could spin around in the cavity of TMeQ[6]. On the other hand, the coexistence of the free and interacted TMeQ[6] leads to a complicated spectrum (Figure 2b) and suggests that weak binding exists between TMeQ[6] and **G2**. The integral of the typical proton of the bound **G2** (such as one pyridyl proton at 8.85 ppm or five phenyl protons at ~6.4 ppm) relative to those of the bound TMeQ[6] (such as H(3)/H(4) at 5.21−5.39 ppm or H(6) at ~3.9 ppm) shows that an inclusion complex could be formed with TMeQ[6] and **G2** in a ratio of 1:1.

No obvious interaction between TMeQ[6] and **G3** can be observed (Figure 3b) until the ratio of the host−guest is increased to 1:25 relative to TMeQ[6] (Figure 3c). Similar to the case of TMeQ[6]-**G2**, the downfield pyridyl proton resonances and upfield phenyl proton resonances suggests a similar

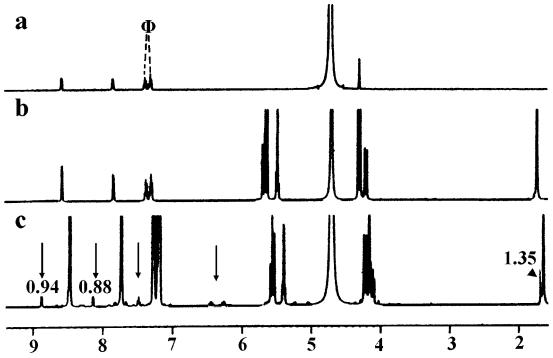

Figure 3. ^{1}H NMR spectra of (a) **G3**, (b) TMeQ[6]-**G3** ($C_{TMeQ[6]}/C_{G3}$ = 1:2.5), and (c) TMeQ[6]-**G3** ($C_{TMeQ[6]}/C_{G3}$ = 1:25). *x* axis: chemical shift (ppm). *y* axis: intensity of resonance. Φ: resonances of phenyl protons of the guest. In (c) the intensities of the corresponding protons are given.

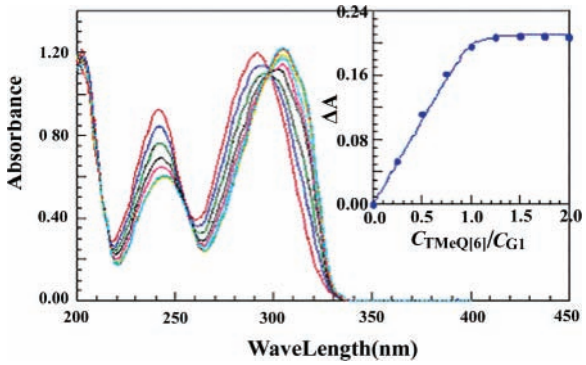

Figure 4. Absorption spectra of TMeQ[6]-**G1** system ($C_{TMeQ[6]}$ = 2.50 × 10^{-5}~2.00 × 10^{-4} mol·L^{-1}). Inset: the corresponding ΔA vs $C_{TMeQ[6]}/C_{G1}$ at 292 nm. Absorption spectrum in the absence of TMeQ[6] (red) and in the presence of 0.25 (blue), 0.50 (light green), and 2.0 (dark green) equiv of TMeQ[6].

inclusion complex, where the phenyl ring is also included in the cavity of TMeQ[6], could be formed.

B. Absorption Spectrophotometric Analysis of the Interaction between TMeQ[6] and Guest Hydrochloride Salts. The ^{1}H NMR spectroscopy discussed above revealed that TMeQ[6] can bind the phenyl moiety of the HCl salt of the three title guests and formed inclusion complexes with a host−guest ratio of 1:1. The significant different upfield shift of the resonances of inner or outer methylene protons and methine protons on TMeQ[6] suggests that the included aromatic group is not symmetrically located in the encapsulating ring. From distributions of the bound and unbound host and guest in the spectra for the different host−guest systems, one can qualitatively estimate the stability of the three pair of host−guest inclusion complexes as TMeQ[6]-**G1** > TMeQ[6]-**G2** > TMeQ[6]-**G3**. However, it was hard to obtain accurate thermodynamic parameters due to the quality of spectra, partly due to the complexity caused by the coexistence of the bound and unbound host and guest. Thus, absorption spectrophotometric analysis has been employed to quantitatively define the interaction between TMeQ[6] and the title guests.

Generally, TMeQ[6] shows no absorbance above ~210 nm, but the absorption bands of **G1** exhibit a progressive red-shift as the ratio of $C_{TMeQ[6]}/C_{G1}$ is increased (Figure 4), while the maximum absorbances of **G1** at λ = 292 nm (A_{292}) become progressively lower with increasing concentration of host from 2.50 × 10^{-5} mol·L^{-1} to 2.00 × 10^{-4} mol·L^{-1}, and the maximum absorbance is red-shifted to λ = 306 nm. The sharp isosbestic points at λ = 256 nm and λ = 298 nm are consistent

with a simple interaction between TMeQ[6] and **G1**. The differences in absorbance (ΔA) vs ratios of mole of the host TMeQ[6] and the guest **G1** ($C_{\text{TMeQ[6]}}/C_{\mathbf{G1}}$) data can be fitted to a 1:1 binding model for the TMeQ[6]-**G1** system at $\lambda_{max} = 292$ nm (see Figure 4 inset), so the 1:1 interaction equilibrium of TMeQ[6] and **G1** is expressed by eq 1:

$$\text{TMeQ[6]} + \mathbf{G1} \xrightarrow{K_{\text{TMeQ[6]}-\mathbf{G1}}} \text{TMeQ[6]-}\mathbf{G1} \qquad (1)$$

The corresponding binding constant ($K_{\text{TMeQ[6]}-\mathbf{G1}}$) was found to be $\sim 2 \times 10^6$ L·mol^{-1} (at 292 nm; $R = 0.999$) by nonlinear least-square fitting according to eq 2. The value determined at a different wavelength did not differ significantly ($\sim 1.9 \times 10^6$ L·mol^{-1} at 246 nm; $R = 0.999$); this was also the case using 10-fold lower concentrations of G1, although absorbance changes are small and K is not well defined.

$$\Delta A = \{\Delta\epsilon([\text{TMeQ[6]}]_0 + [\mathbf{G1}]_0 + 1/K_a) \pm \sqrt{\Delta\epsilon^2([\text{TMeQ[6]}]_0 + [\mathbf{G1}]_0 + 1/K_a)^2 - 4\Delta\epsilon^2[\text{TMeQ[6]}]_0[\mathbf{G1}]_0}\}/2 \qquad (2)$$

where ΔA is the change in the absorbance of guest on gradual addition of TMeQ[6], whereas $\Delta\epsilon$ refers to the difference of molar absorptivity between complexed and free **G1**; the total concentration of TMeQ[6] and guest is denoted by $[\text{TMeQ[6]}]_0$ and $[\mathbf{G1}]_0$.

The absorption spectra of free **G2** or **G3** are almost the same as those of the mixture of TMeQ[6] and **G2** or **G3** combined in a ratio of 1:1 (Figure S1, Supporting Information) due to the relatively small association constants in those cases. Therefore, it is not possible to obtain accurate binding constants for the TMeQ[6]-**G2** or TMeQ[6]-**G3** systems by using the above titration method. However, the subtle difference between the absorbances of free **G2** or **G3** and the bound **G2** or **G3** by the host TMeQ[6] is adventitious because it allows the method developed below to be employed successfully for defining the binding constants for the TMeQ[6]-**G2** or TMeQ[6]-**G3** systems by a different approach.

Thus, competitive interaction of the guest **G1** with the host−guest TMeQ[6]-**G2** or TMeQ[6]-**G3** was employed, the competition given by

$$\mathbf{G_1} + \text{TMeQ[6]-}\mathbf{G}\boldsymbol{n} \rightleftharpoons \mathbf{G}\boldsymbol{n} + \text{TMeQ[6]-}\mathbf{G_1} \qquad (3)$$

where $\mathbf{G}\boldsymbol{n} = \mathbf{G2}$ or **G3**, with the equilibrium constant K defined by

$$K = (C_{\text{TMeQ[6]}-\mathbf{G1}} \cdot C_{\mathbf{G}\boldsymbol{n}})/(C_{\text{TMeQ[6]}-\mathbf{G}\boldsymbol{n}} \cdot C_{\mathbf{G1}}) \qquad (4)$$

Two independent equilibria of TMeQ[6] + **G1** ⇌ TMeQ[6]-**G1** ($K_{\text{TMeQ[6]}-\mathbf{G1}}$) and TMeQ[6] + $\mathbf{G}\boldsymbol{n}$ ⇌ TMeQ[6]-**Gn** ($K_{\text{TMeQ[6]}-\mathbf{Gn}}$) could be considered in the competitive interaction, thus, eq 4 can be rearranged:

$$K = (C_{\text{TMeQ[6]}-\mathbf{G1}} \cdot C_{\mathbf{G}\boldsymbol{n}}) \cdot C_{\text{TMeQ[6]}} / (C_{\text{TMeQ[6]}-\mathbf{G}\boldsymbol{n}} \cdot C_{\mathbf{G1}}) \cdot C_{\text{TMeQ[6]}} = K_{\text{TMeQ[6]}-\mathbf{G1}}/K_{\text{TMeQ[6]}-\mathbf{G}\boldsymbol{n}} \qquad (5)$$

or

$$K_{\text{TMeQ[6]}-\mathbf{G}\boldsymbol{n}} = K_{\text{TMeQ[6]}-\mathbf{G1}}/K \qquad (6)$$

If we use the solution of TMeQ[6]-**G2** or TMeQ[6]-**G3** with combined host and guest in a ratio of 1:1 as the blank, due to no significant difference between the absorption bands of the bound and unbound **G2** or **G3**, the absorbance of the competitive system should be attributed to the absorbances of the free **G1**($A_{\mathbf{G1}}$) and the host−guest inclusion complex of TMeQ[6]-**G1**($A_{\text{TMeQ[6]}-\mathbf{G1}}$) with the same concentration as that of **G2** or **G3**, and the observed equilibrium constant K could be obtained from kinetic methods. Figure 5 shows plots of absorbances (A) vs time(s) for the competitive interactions of **G1**-TMeQ[6]**G2** and **G1**-TMeQ[6]**G3**.

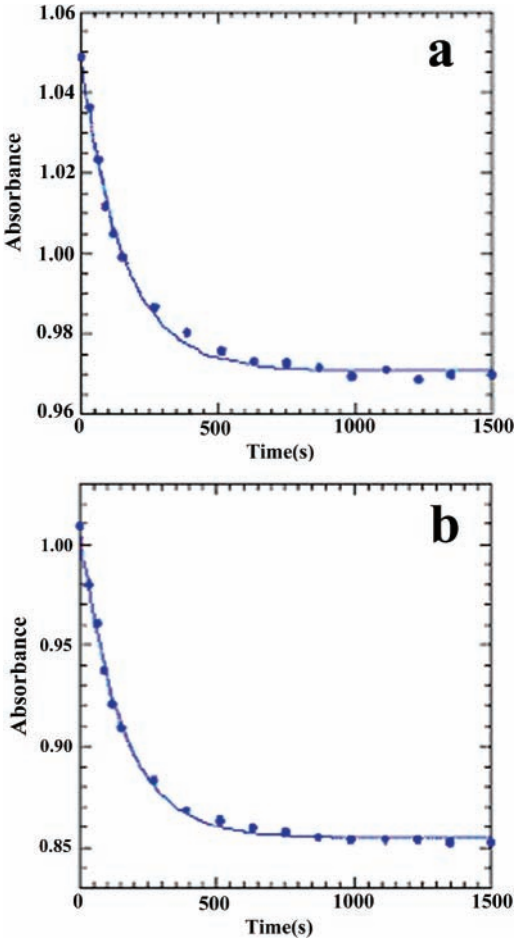

Figure 5. Plots of absorbances (**A**) vs time(s) for the two competitive interactions (a) $C_{\text{TMeQ[6]}\mathbf{G2}}/C_{\mathbf{G1}} = 1{:}1$; (b) $C_{\text{TMeQ[6]}\mathbf{G3}}/C_{\mathbf{G1}} = 1{:}1$.

The detailed kinetics reveals that both observed rate constants $K_{\mathbf{G1}-\text{TMeQ[6]}\mathbf{G2}}$ or $K_{\mathbf{G1}-\text{TMeQ[6]}\mathbf{G3}}$ followed pseudo-first-order behavior, with equations:

$$A_{\mathbf{G1}-\text{TMeQ[6]}\mathbf{G2}} = 0.97112 + 0.07697 \times \exp(-K_{\mathbf{G1}-\text{TMeQ[6]}\mathbf{G2}} \cdot t); \quad K_{\mathbf{G1}-\text{TMeQ[6]}\mathbf{G2}} = 6.46 \times 10^{-3}\ \text{s}^{-1} \qquad (7)$$

$$A_{\mathbf{G1}-\text{TMeQ[6]}\mathbf{G3}} = 0.85513 + 0.15322 \times \exp(-K_{\mathbf{G1}-\text{TMeQ[6]}\mathbf{G3}} \cdot t); \quad K_{\mathbf{G1}-\text{TMeQ[6]}\mathbf{G3}} = 6.65 \times 10^{-3}\ \text{s}^{-1} \qquad (8)$$

From eqs 7 and 8, the half-life (τ) of the competitive interactions of **G1**-TMeQ[6]**G2** and **G1**-TMeQ[6]**G3** can be calculated, being 108 and 103 s, respectively.

Thus, the absorbance of the competitive interaction system (A_τ) at half-life (τ) is given by

$$A_\tau = A_{\mathbf{G1}} \times 50\% + A_{\text{TMeQ[6]}-\mathbf{G1}} \times 50\% \qquad (9)$$

and the $A_{\text{TMeQ[6]}-\mathbf{G1}}$ can be calculated using eq 7 and the molar

absorptivity ($\epsilon_{TMeQ[6]-G1}$) can be calculated using eq 8:

$$\epsilon_{TMeQ[6]-G1} = A_{TMeQ[6]-G1}/C_0 \qquad (10)$$

$$C_0 = 2.00 \times 10^{-4}\ \text{mol·L}^{-1}$$

When equilibrium is reached, the absorbance of the competitive interaction (A_∞) is given by

$$A_\infty = [x\cdot\epsilon_{TMeQ[6]-G1} + (1-x)\cdot\epsilon_{G1}]\cdot C_0 \qquad (11)$$

where x is the proportion of **G1** that has formed the inclusion complex TMeQ[6]-**G1** to the total concentration of **G1** in the competitive interaction and can be calculated using eq 11. Thus, the observed equilibrium constant K can be calculated using eq 4, and then the binding constants $K_{TMeQ[6]-G2}$ and $K_{TMeQ[6]-G3}$ for the inclusion complex of TMeQ[6]-**G2** or TMeQ[6]-**G3** can be calculated using eq 6; they are 60.7 mol^{-1}·L and 19.9 mol^{-1}·L, respectively, a significant difference compared to that of TMeQ[6]-**G1** ($K_{TMeQ[6]-G1} \sim 2 \times 10^6$ L·mol^{-1}).

Thus, we have established a competitive interaction, in which one host−guest inclusion complex pair, such as TMeQ[6]-**G1**, is much more stable than another host−guest inclusion complex pair, such as TMeQ[6]-**G2** or TMeQ[6]-**G3**. Fortunately, only subtle differences between the absorption spectra of the bound and unbound **G2** or **G3** provides an opportunity to simplify the process to obtain the related thermodynamic parameters.

The significant difference between stability constants for the three host−guest inclusion complexes of TMeQ[6]-**G1** compared with TMeQ[6]-**G2** and TMeQ[6]-**G3**, of the order of $\sim 10^5$, is notable. The presence of an additional methylene between the two aromatic rings in **G2** and **G3** compared with **G1** is clearly a key. This means that the external pyridinium nitrogen is displaced further from the surrounding carbonyl oxygens, limiting opportunities for hydrogen bonding which presumably stabilize the complex and affect the driving force for assembly of the inclusion complex. Positioning the N further away, as in **G3**, reduces the driving force further. The clear variation in hydrogen bonding interactions identified in modeling the three docked systems below is notable and suggests that establishing such linkages in a transition state may be particularly important.

C. Molecular Geometry Simulation of TMeQ[6] and Its Inclusion Complexes. Above, we investigated the interactions between TMeQ[6] and three selected guests by using ^{1}H NMR and absorption spectrophotometric analysis. The ^{1}H NMR spectroscopy established an interaction model of the host−guest complexes in which the phenyl moiety of the title guests is included in the cavity of the TMeQ[6] and the ^{1}H NMR spectra analysis reveals qualitatively the stability of the title host−guest inclusion complexes. The absorption spectrophotometric analysis permitted quantitative determination of thermodynamic properties for the title host−guest inclusion complexes. However, when one looks at the structure of the three phenyl- or benzyl-substituted pyridine guests, although no major difference exists between them except for a methylene existing between the two aromatic ring in **G2** or **G3**, it nevertheless leads to a significant difference in the stability of the three host−guest inclusion complexes. To understand how a subtle difference in the structure of the guests leads to a significant difference in the stability of the corresponding host−guest inclusion complexes with TMeQ[6], reasonable level ab initio theoretical methods have been performed for the gas phase and also extended to the solution phase (water as solvent) in the cases.

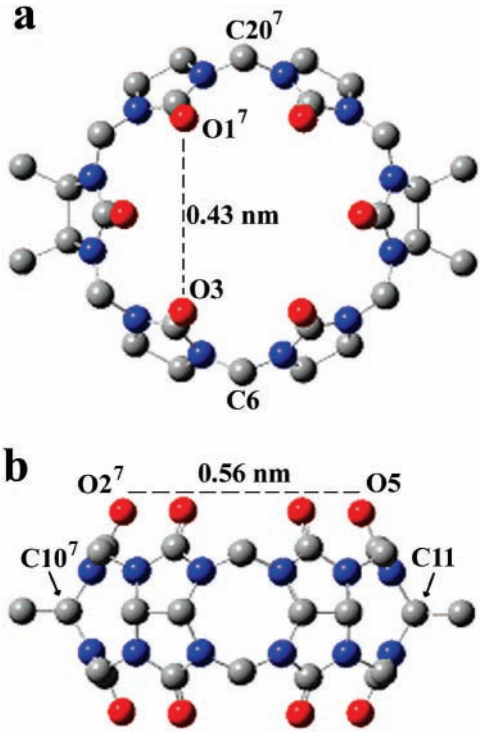

Figure 6. Bird's-eye (a) and side view (b) of TMeQ[6] model.

The geometry of TMeQ[6] was optimized with HF/3-21G* basis sets and is displayed in Figure 6. It was surprising to find that the macrocycle was not strictly circular but ellipsoidal. The distance between the portal oxygens O1^7 and O3 is ~0.43 nm, whereas the distance between the portal oxygens O2 and O5 is ~0.56 nm. The calculated structure, with an ellipsoid of D_{2h} symmetry, is supported by the result of single-crystal X-ray diffraction.[17] The inner cavity distances of unsubstituted Q[6] (0.84 nm) can be compared to distances between the cavity carbons C20^7 and C6 (~0.81 nm), while the distance between the cavity carbons C10^7 and C11 is ~0.92 nm, approximately 14% larger than that of the closer sides.

The pregeometry optimized structures for the host−guest inclusion complexes using the anneal method within the MM+ force field in the gas revealed that, when the phenyl moiety of the three pyridine derivate guest was included, the host−guest complexation reached a minimum. The charged guest was established using the Hyperchem release 7.52 package, and the charge balance anion Cl^- in host−guest complexes was omitted. On the basis of the minimum, the further optimized structures for the host−guest inclusion complexes at HF/3-21G* level are shown in Figure 7 and the corresponding energy differences for the formation of the title host−guest inclusion complexes and related structural parameters are shown in Table 1.

Generally, cucurbit[n]urils and their derivates form stable inclusion complexes with guests through a combination of dipole−ion, hydrogen bonding, and hydrophobic interactions. In this work, it is common that a hydrophobic interaction occurs in each related host−guest inclusion complex because the experimental and calculated results unambiguously demonstrate same-cavity binding, i.e., the phenyl moiety of all three pyridine derivate guests enters the cavity of the host TMeQ[6] when they interact each other. Therefore, the dipole−ion hydrogen bonding involved in the portal interaction could be the reason leading to the significant difference in the stability of the three host−guest inclusion complexes. Principally, the protonation of the nitrogen on the pyridine moiety of the guests offer an opportunity to form some hydrogen bonds with the carbonyl

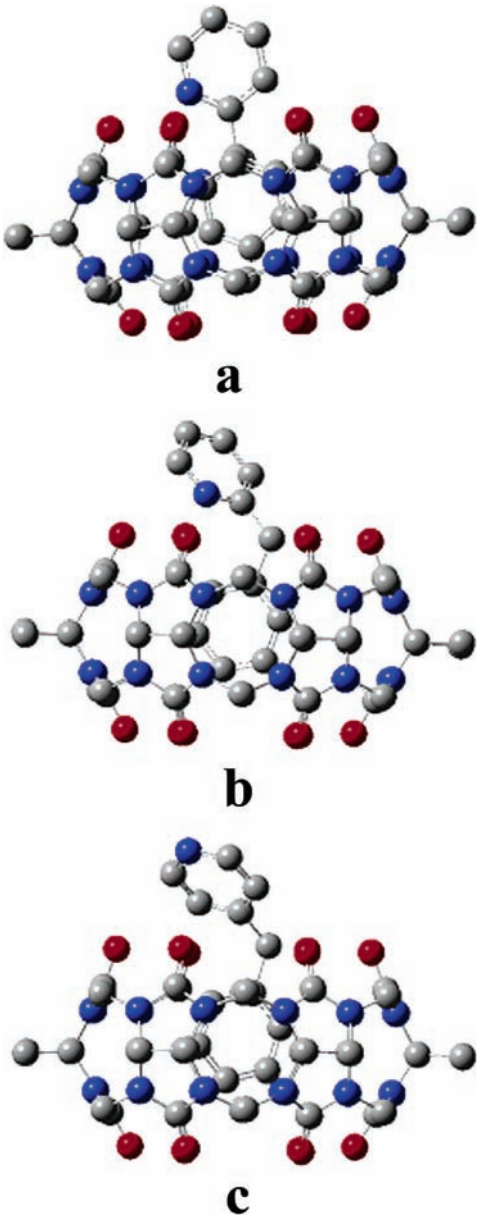

Figure 7. Lowest energy geometries of complexes.

TABLE 1: Character Value of Inclusion Complexes

		Q + G1 → Q-G1	Q + G2 → Q-G2	Q + G3 → Q-G3
ΔE (kJ·mol^{-1})	in gas	−287.62	−287.42	−232.48
	in water	−283.93	−279.54	−211.01
θ (deg)		15.39	15.21	19.83
$K_{Q-Gi(i=1-3)}$ (L·mol^{-1})		2.0×10^6	60.72	19.93

oxygen on one portal of the host TMeQ[6], and the strength of the hydrogen bonds is dependent on the distances between the related atoms. The optimized structure of the complex of TMeQ[6]-**G1** has three $N_{pyridyl}-O_{carbonyl}$ distances (2.68, 2.86, and 2.95 Å) within hydrogen-bonding length. By comparison, although three $N_{pyridyl}-O_{carbonyl}$ distances are found within the hydrogen bond length for the complex of TMeQ[6]-**G2**, they are 2.70, 2.94, and 3.64 Å, respectively, and longer than those in TMeQ[6]-**G1**. For TMeQ[6]-**G3**, only two $N_{pyridyl}-O_{carbonyl}$ distances (3.30, 3.99, Å) could be within the hydrogen bond length. Moreover, in the case of the charged ammonium or pyridine guest, the host−guest complex is held together by additional ion−dipole interactions between the positive charged

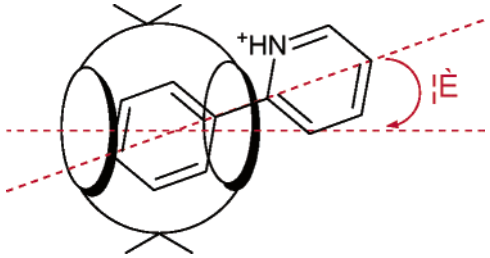

Figure 8. Schematic representation of θ angle in guest-TMeQ[6] system.

group and the ureido carbonyl oxygens. We assumed that, if the pathway for ingression of the phenyl moiety of the guests is along the TMeQ[6] rotational symmetry axis, the θ angle (Figure 8) is dependent upon the particular guest for the three host−guest inclusion complexes. For **G1 or G2**, the position of the charged nitrogen on the pyridine moiety is suitable for forming both hydrogen bonds and dipole−ion interaction with the carbonyl oxygens, and the computed θ angles are almost the same (referring to Table 1). For **G3**, the position of the charged nitrogen on the pyridine moiety is further away from the portal of the TMeQ[6], and the charged nitrogen is bent further from the carbonyl oxygens in the inclusion complex of TMeQ[6]-**G3** because a bigger θ angle is observed (refer to Table 1). Thus, the three host−guest inclusion complexes in this work demonstrate again both cavity and portal binding, with the stability of the complexes investigated qualitatively and quantitatively.

On the other hand, the negative differences of the energy minima between the free host, free guest, and the host−guest inclusion complex ($\Delta E < 0$) reveal that the host TMeQ[6] favors inclusion of the guests via the two important supramolecular interactions, namely a hydrophobic effect and the portal interaction, which mainly involve the dipole−ion interaction and the hydrogen bonding. The order of energy differences (ΔE) show a qualitatively agreement with the order of the stability of the title host−guest inclusion complexes.

Conclusion

The present study on interaction between tetramethylcucurbit-[6]uril with three pyridine derivatives that have two moieties have been investigated by using ^{1}H NMR spectroscopy and electronic absorption spectroscopy and theoretical calculations. The ^{1}H NMR spectra analysis established a basic interaction model in which the host selectively binds the phenyl moiety of the HCl salt of the above three guests and formed the inclusion complexes with a host−guest ratio of 1:1. Absorption spectrophotometric analysis allowed the stability of these host−guest inclusion complexes to be determined quantitatively. Particularly, we have established a competitive interaction in which one host−guest inclusion complex pair is much more stable than another host−guest inclusion complex pair. The stability constants for the three host−guest inclusion complexes of TMeQ[6]-**G1**, TMeQ[6]-**G2**, and TMeQ[6]-**G3** are 2.0×10^6 mol^{-1}·L, 60.7 mol^{-1}·L, and 19.9 mol^{-1}·L, respectively. To understand how subtle differences in the structure of the title guests lead to a significant difference in the stability of the corresponding host−guest inclusion complexes with the TMeQ-[6], ab initio theoretical calculations have been performed for the gas phase and also the solution phase (water as solvent) in all cases. The pregeometry optimized structures for the host−guest inclusion complexes were performed by using the anneal method within the MM+ force field in gas; further optimized

structures for the host−guest inclusion complexes were calculated at HF/3-21G* level. The calculation results revealed that, when the phenyl moiety of the three pyridine derivate guest was included, the host−guest complexation reached the minimum, and the corresponding energy differences for the formation of the title host−guest inclusion complexes are consistent with the experimental results.

Acknowledgment. We acknowledge the support of Excellence Young Teacher Program of the Chinese Ministry of Education (EYTP), National Natural Science Foundation of China (grant nos. 200261002, 20362003), International Collaborative Project of the Chinese Ministry of Science and Technology (grant no. 2003DF000030), and the Governor Foundation of Guizhou Province.

Supporting Information Available: Absorption spectra of **G2**, TMeQ[6]-**G2**, and **G3**, TMeQ[6]-**G2** ($C_{\mathbf{G2}} = C_{\mathbf{G3}} = C_{\mathrm{TMeQ[6]-G2\ or\ 3}} = 2.00 \times 10^{-4}$ mol·L^{-1}). This material is available free of charge via the Internet at http://pubs.acs.org.

References and Notes

(1) Lagona, J.; Mukhopadhyay, P.; Chakrabarti, S.; Isaacs, L. *Angew. Chem., Int. Ed.* **2005**, *44*, 4844.

(2) Lee, J. W.; Samal, S.; Selvapalam, N.; Kim, H. J.; Kim, K. *Acc. Chem. Res.* **2003**, *36*, 621.

(3) Gerasko, O. A.; Samsonenko, D. G.; Fedin, V. P. *Russ. Chem. Rev.* **2002**, *71*, 741.

(4) Elemans, J. A. A. W.; Rowan, A. E.; Nolte, R. J. M. *Ind. Eng. Chem. Res.* **2000**, *39*, 3419.

(5) Hubin, T. J.; Kolchinski, A. G.; Vance, A. L.; Busch, D. H. *Adv. Supramol. Chem.* **1999**, *5*, 237.

(6) Mock, W. L. *Top. Curr. Chem.* **1995**, *175*, 1.

(7) Cintas, P. *J. Inclusion Phenom. Mol. Recognit. Chem.* **1994**, *17*, 205.

(8) Freeman, W. A.; Mock, W. L. *J. Am. Chem. Soc.* **1981**, *103*, 7367.

(9) Day, A. I.; Arnold, A. P. Method for Synthesis of Cucurbiturils. Patent WO 0068232, 2000, *8*.

(10) Kim, J.; Jung, I.-S.; Kim, S.-Y.; Lee, E.; Kang, J.-K.; Sakamoto, S.; Yamaguchi, K.; Kim, K. *J. Am. Chem. Soc.* **2000**, *122*, 540.

(11) Day, A. I.; Blanck, R. J.; Arnold, A. P.; Lorenzo, S.; Lewis, G. R.; Dance, I. *Angew. Chem., Int. Ed.* **2002**, *41*, 275.

(12) Zhao, J.; Kim, H.-J.; Oh, J.; Kim, S.-Y.; Lee, J. W.; Sakamoto, S.; Yamaguchi, K.; Kim, K. *Angew. Chem., Int. Ed.* **2001**, *40*, 4233.

(13) Flinn, A.; Hough, G. C.; Stoddart, J. F.; Williams, D. J. *Angew. Chem., Int. Ed. Engl.* **1992**, *31*, 1475.

(14) Isobe, H.; Sato, S.; Nakamura, E. *Org. Lett.* **2002**, *4*, 1287.

(15) Day, A. I.; Arnold, A. P.; Blanch, R. J. *Molecules* **2003**, *8*, 74.

(16) Sasmal, S.; Sinha, M. K.; Keinan, E. *Org. Lett.* **2004**, *6*, 1225.

(17) Zhao, Y.-J.; Xue, S.-F.; Zhu, Q.-J.; Tao, Z.; Zhang, J.-X.; Wei, Z.-B.; Long, L.-S.; Hu, M.-L.; Xiao, H.-P.; Day, A. I. *Chin. Sci. Bull.* **2004**, *49*, 1111.

(18) Zheng, L.; Zhu, J.; Zhang, Y.; Tao, Z.; Xue, S.; Zhu, Q.; Wei, Z.; Long, L. *Chin. J. Inorg. Chem.* **2005**, *21*, 1583.

(19) Zhao, Y.-J.; Xue, S.-F.; Zhang, Y.-Q.; Zhu, Q.-J.; Tao, Z.; Zhang, J.-X.; Wei, Z.-B.; Long, L.-S. *Acta Chim. Sin.* **2005**, *63*, 913.

(20) Jon, S. Y.; Selvapalam, N.; Oh, D. H.; Kang, J.-K.; Kim, S.-Y.; Jeon, Y. J.; Lee, J. W.; Kim, K. *J. Am. Chem. Soc.*, **2003**, *125*, 10186.

(21) Wagner, B. D.; Boland, P. G.; Lagona, J.; Isaacs, L. *J. Phys. Chem. B* **2005**, *109*, 7686.

(22) Lagona, J.; Fettinger, J. C.; Issacs, L. *J. Org. Chem.* **2005**, *70*, 10381.

(23) Lagona, J.; Wagner, B. D.; Isaacs, L. *J. Org. Chem.* **2006**, *71*, 1181.

(24) Miyahara, Y.; Goto, K.; Oka, M.; Inazu, T. *Angew. Chem., Int. Ed. Engl.* **2004**, *43*, 5019.

(25) Issacs, L.; Park, S.-K.; Liu, S.; Ko, Y. H.; Selvapalam, N.; Kim, Y.; Kim, H.; Zavalij, P. Y.; Kim, G.-H.; Lee, H.-S.; Kim, K. *J. Am. Chem. Soc.* **2005**, *127*, 1800.

(26) Mock, W. L.; Shih, N.-Y. *J. Org. Chem.* **1986**, *51* 4440.

(27) Mock, W. L.; Shih, N.-Y. *J. Org. Chem.* **1988**, *110*, 4760.

(28) Mock, W. L.; Shih, N.-Y. *J. Am. Chem. Soc.* **1989**, *111*, 2697.

(29) Meschke, H.-J.; Buschmann, E.; Schollmeyer, E. *Thermochim. Acta* **1997**, *297*, 43.

(30) Wagner, B. D.; Stojanovic, N.; Day, A. I.; Blanch, R. J. *J. Phys. Chem. B* **2003**, *107*, 10741.

(31) Zhang, K.-C.; Mu, T.-W.; Liu, L.; Guo, Q.-X. *Chin. J. Chem.* **2001**, *19*, 558.

(32) Ong, W.; Gómez-Kaifer, M.; Kaifer, A. E. *Org. Lett.* **2002**, *4*, 1791.

(33) Ong, W.; Kaifer, A. E.; *Angew. Chem.* **2003**, *42*, 2164.

(34) Ong, W.; Kaifer, A. E. *J. Org. Chem.* **2004**, *69*, 1383.

(35) Moon, K.; Kaifer, A. E. *Org. Lett.* **2004**, *6*, 185.

(36) Fu, H.; Xue, S.; Mu, L.; Du, Y.; Zhu, Q.; Tao, Z.; Zhang, J.; Day, A. I. *Sci. China Ser. B* **2004**, *34*, 517.

(37) Fu, H.-Y.; Xue, S.-F.; Zhu, Q.-J.; Tao, Z.; Zhang, J.-X.; Day, A. I. *J. Inclusion Phenom. Macrocyclic Chem.* **2005**, *52*, 101.

(38) Liu, J.-X.; Tao, Z.; Xue, S.-F.; Zhu, Q.-J.; Zhang, J.-X. *Chin. J. Inorg. Chem.* **2004**, *20*, 139.

(39) Hyperchem, release 7.52 for Windows Molecular Modeling System, Hypercube, Inc.

(40) Frisch, M. J.; Trucks, G. W.; Schlegel, H. B.; Scuseria, G. E.; Robb, M. A.; Cheeseman, J. R.; Montgomery, J. A., Jr.; Vreven, T.; Kudin, K. N.; Burant, J. C.; Millam, J. M.; Iyengar, S. S.; Tomasi, J.; Barone, V.; Mennucci, B.; Cossi, M.; Scalmani, G.; Rega, N.; Petersson, G. A.; Nakatsuji, H.; Hada, M.; Ehara, M.; Toyota, K.; Fukuda, R.; Hasegawa, J.; Ishida, M.; Nakajima, T.; Honda, Y.; Kitao, O.; Nakai, H.; Klene, M.; Li, X.; Knox, J. E.; Hratchian, H. P.; Cross, J. B.; Bakken, V.; Adamo, C.; Jaramillo, J.; Gomperts, R.; Stratmann, R. E.; Yazyev, O.; Austin, A. J.; Cammi, R.; Pomelli, C.; Ochterski, J. W.; Ayala, P. Y.; Morokuma, K.; Voth, G. A.; Salvador, P.; Dannenberg, J. J.; Zakrzewski, V. G.; Dapprich, S.; Daniels, A. D.; Strain, M. C.; Farkas, O.; Malick, D. K.; Rabuck, A. D.; Raghavachari, K.; Foresman, J. B.; Ortiz, J. V.; Cui, Q.; Baboul, A. G.; Clifford, S.; Cioslowski, J.; Stefanov, B. B.; Liu, G.; Liashenko, A.; Piskorz, P.; Komaromi, I.; Martin, R. L.; Fox, D. J.; Keith, T.; Al-Laham, M. A.; Peng, C. Y.; Nanayakkara, A.; Challacombe, M.; Gill, P. M. W.; Johnson, B.; Chen, W.; Wong, M. W.; Gonzalez, C.; Pople, J. A. *Gaussian 03*, revision C.02; Gaussian, Inc.: Wallingford, CT, 2004.